Transfer of ice algae carbon to ice-associated amphipods in the high-Arctic pack ice environment

Thomas A. Brown[1,2*], Philipp Assmy[3], Haakon Hop[3,4], Anette Wold[3] and Simon T. Belt[2]

[1] Marine Ecology and Chemistry, Scottish Association for Marine Science, Oban, Argyll, UK, PA37 1QA.

[2] School of Geography, Earth and Environmental Sciences, University of Plymouth, Plymouth PL4 8AA, UK

[3] Norwegian Polar Institute, Fram Centre, N-9296 Tromsø, Norway

[4] Department of Arctic and Marine Biology, Faculty of Biosciences, Fisheries and Economics, UiT The Arctic University of Norway, N-9037 Tromsø, Norway

[*] Corresponding author: Thomas.Brown@sams.ac.uk

ABSTRACT

Sympagic (ice-associated) amphipods channel carbon into the marine ecosystem. With Arctic sea ice extent in decline, it is becoming increasingly important to quantify this transfer of sympagic energy. Recently, a method for quantifying sympagic particulate organic carbon (iPOC) in filtered water samples was proposed based on the abundances of the Arctic sea ice biomarker IP_{25}. Here, we tested the hypothesis that adoption of this method could also provide quantitative estimates of iPOC transfer within Arctic amphipods. We analysed five amphipod species collected north of Svalbard and compared findings to some previous studies. Estimates showed that *Onisimus glacialis* and *Apherusa glacialis* contained the most iPOC, relative to dry mass (23.5 ± 4.5 and 9.8 ± 1.9 mg C g^{-1}, respectively), while *Gammarus wilkitzkii* had the highest grazing impact on the available ice algae (0.48 mg C m^{-2}, for an estimated 24 h), equating to 73% of algal standing stock. Our findings are also broadly consistent with those obtained by applying the H-Print biomarker approach to the same samples. The ability to obtain realistic quantitative estimates of iPOC into sympagic and pelagic fauna will likely have important implications for modelling energy flow in Arctic food webs during future climate scenarios.

KEYWORDS: Arctic amphipods, organic carbon, IP_{25}, H-Print, Nansen Basin

INTRODUCTION

Arctic sea ice provides a unique habitat for ice-associated algae, in particular diatoms (Dieckmann and Hellmer, 2010; Leu *et al.*, 2015), which offer food for a wide range of heterotrophic organisms, with some of the most noticeable being certain crustaceans (Arrigo, 2014) such as copepods, decapods, euphausiids and amphipods (Arndt and Swadling, 2006). In Arctic waters, analyses of baited traps and sediment traps have demonstrated that amphipods can dominate biomass in such settings (Nygård *et al.*, 2009; Kraft *et al.*, 2010) and so, in turn, provide an important link between sea ice algae and intermediary, as well as higher trophic level consumers, including fish, seabirds and marine mammals (Lønne and Gabrielsen, 1992; Lønne and Gulliksen, 1989; Dalpadado *et al.*, 2016). With Arctic sea ice extent receding (Serreze *et al*., 2016), there is a growing need to understand the impact of potential changes in the timing, magnitude and composition of ice algal blooms and the consequences for sympagic, pelagic and benthic grazers (Søreide *et al.*, 2013; Leu *et al.*, 2015), since ice-associated amphipods are particularly sensitive to changes in sea ice conditions related to climate change (Kraft *et al.*, 2010; Barber *et al.*, 2015).

The direct coupling between sympagic (i.e. sea ice associated) and pelagic communities has been demonstrated recently following the identification of the Arctic sea ice diatom biomarker IP_{25} (Fig. 1; Belt *et al*., 2007) in ice-associated zooplankton during springtime (Brown and Belt, 2012a). IP_{25} is a highly branched isoprenoid (HBI) lipid that serves as a selective tracer of ice-derived organic matter since it is only biosynthesized by certain Arctic sympagic diatoms (Belt *et al*., 2007; Brown *et al*., 2014c). Although these particular diatoms are generally the minority species, they are, nonetheless, pan-Arctic in distribution (Brown *et al.*, 2014c). The presence and abundance of IP_{25} in Arctic sea ice correlate well with spring sea ice diatom biomass (Brown *et al.*, 2011), which has led to the use of this lipid as a qualitative biomarker for sea ice particulate organic carbon (iPOC)

(Brown *et al.*, 2016). Consistent with this, IP_{25} has been identified in sinking iPOC (Belt *et al.*, 2008; Brown, 2011; Brown *et al.*, 2016), sediments (Belt and Müller, 2013) and animals (Brown *et al.*, 2014a, 2015; Brown and Belt, 2012b) across the Arctic.

In a previous case study investigation, the quantification of IP_{25} in bulk zooplankton from the Amundsen Gulf (Beaufort Sea) between February and June 2008, demonstrated further that analysis of IP_{25} represents a potentially useful method for confirming the link between ice algae and heterotrophs (Brown and Belt, 2012a). During the sampling period, increases in the grazing impact of zooplankton were inferred based on higher IP_{25} concentrations within zooplankton, signifying an increase in ice algal grazing. However, a more thorough understanding of the effects of declining sea ice thickness and extent, and therefore sympagic algae, on Arctic animals requires more detailed quantification of sympagic carbon consumption, which, until recently, has not been achievable from IP_{25} concentration data alone. However, a more recent study demonstrated that concentrations of IP_{25} measured in seawater beneath sea ice during the spring melt can be used to obtain quantitative estimates of sinking iPOC (Brown *et al.*, 2016). In essence, quantitative estimates of iPOC in the water column were obtained by combining respective IP_{25} concentrations with the iPOC/IP_{25} ratio derived from analysis of the overlying sea ice. Using this approach, Brown *et al*. (2016) showed that iPOC accounted for up to 100% of the total organic carbon available to consumers in the upper water column at the time when sympagic algae were being released from the ice matrix.

Combined, the previous identification of IP_{25} in zooplankton (Brown and Belt, 2012a) and the recent demonstration that iPOC could be quantified in the water column (Brown *et al.*, 2016), led us to hypothesise that a similar approach could be used to quantify iPOC in Arctic primary consumers, such as some amphipod species that are known to graze on ice algae. Here, we tested this hypothesis by 1) determining the iPOC/IP_{25} ratio within ice algal

aggregates collected beneath sea ice, north of Svalbard in the Nansen Basin, 2) quantifying IP_{25} in amphipods sampled from beneath sea ice that were observed feeding on ice algae, and 3) combining these findings to quantify iPOC in amphipods. Having established a means of quantifying iPOC in amphipods, our aim was to provide the first quantitative estimates of iPOC consumption for *in-situ* ‘autochthonous’ (permanently inhabiting sea ice) amphipod species; *Gammarus wilkitzkii* Fabricius, 1775, *Apherusa glacialis* Hansen, 1887, *Onisimus nanseni* Sars, 1900, *Onisimus glacialis* Sars, 1900 and the ‘allochthonous’ (partly ice-associated) amphipod, *Eusirus holmi* Hansen, 1887. To complement the iPOC/IP_{25} approach, we also calculated the so-called H-Print (Brown *et al*., 2014d; Brown and Belt, 2017) for each sample, a method that combines the relative abundances of a variety of diatom-derived HBIs, and has been adopted previously to provide semi-quantitative estimates of the proportion of sympagic versus pelagic carbon in zooplankton (Brown and Belt, 2017) fish, seals and marine mammals (Brown *et al*., 2017).

METHOD

Site description and sample collections

The area of sample collection was in the Nansen Basin north of Nordaustlandet, Svalbard (Fig. 2). Ice algal aggregates and ice-associated amphipods were collected at an ice-station during the ICE12 expedition in July 2012, where the Norwegian Polar Institute research vessel *Lance* was moored to a large drifting ice floe at starting point 82.5°N, 21°E. The drift was southward towards the outer margins of the marginal ice zone (Fig. 2). The sea ice comprised mainly first-year ice and extended over a region where the water depth was up to 2500 m.

Sampling of ice algal aggregates

Floating ice algal aggregates were collected with a coarse-meshed sieve through a specially drilled ice hole (3.2 m^2 in size) at 12 h intervals from 29 July − 1 August 2012 (for more details see Assmy *et al.*, 2013). Upon return to the ship, ice algal aggregates were transferred into 50 mL centrifuge tubes and frozen at -20ºC.

Sampling of amphipods

Samples of amphipods were collected on 24 separate occasions from 28 July − 1 August 2012 below the ice by scuba divers using an electrical suction pump with a 500 µm mesh net (Lønne, 1988). Qualitative sampling of amphipods for IP_{25} analysis was carried out by sampling as many organisms as possible during 40−60 min of diving. The amphipods were sorted by species and frozen at -80 °C in zip-lock plastic bags.

Quantitative amphipod sampling was carried out by scuba divers using 50 × 50 cm standard frames (Hop *et al.*, 2000). Electrical suction pumps were used to collect samples from a set area of flat or ridged sea ice by placing these frames 10 times (one replicate sample) in a direction from the dive hole where ice amphipods occurred and exhaled bubbles were absent. Replicates (5 per flat or ridged sea ice) were taken by a single diver in different directions from the dive hole to avoid repeated sampling of the same under-ice area. The samples were preserved in buffered formaldehyde solution at a final concentration of 4% and were subsequently analysed for species composition, abundance and biomass at the Institute of Oceanology, Sopot, Poland. The total length of amphipods was determined from formaldehyde-preserved organisms blotted on filter paper. Abundance estimates (per m^2) were made based on the area covered for each replicate sample (2.5 m^2).

Total organic carbon

Sub-samples (~50 mg) of freeze-dried algae were decarbonated (10% HCl; 10 mL), washed (3 × 10 mL Milli-Q water) and freeze-dried prior to analysis using a Thermoquest EA1110 CHN analyser. L-cystine was used as a calibration standard.

Lipid extraction and purification

Extraction of HBI lipids from freeze-dried algae and amphipods was carried out using established techniques (Belt *et al.*, 2012; Brown *et al.*, 2014d). An internal standard (9-octylheptadec-8-ene (9-OHD); 10 µL; 2 µg mL^{-1}) was added to enable the quantification of IP_{25} (Belt *et al.*, 2012). Samples were covered in methanol (4 mL) and amphipods were mechanically crushed using a glass rod. Samples were then sonicated for 10 min. Milli-Q water (1 mL) and hexane (3×4 mL) were added, and then solutions were vortexed (1 min) and centrifuged (2 min; 2500 revolutions min^{-1}). Supernatant solutions containing lipids were transferred to clean vials with glass pipettes and dried (N_2 stream). Extracts were then re-suspended in hexane (1 mL) and fractionated, providing non-polar lipids (IP_{25} and other HBIs) using column chromatography (5 mL hexane; SiO_2; 0.5 g).

Lipid analysis

Analyses of purified non-polar lipid extracts containing IP_{25} and other HBIs were carried out using gas chromatography–mass spectrometry (GC–MS) (Belt *et al.*, 2012). Total ion current (TIC) chromatograms were used to determine the retention times and mass spectra of HBIs, and these were compared with those of authentic standards (Belt *et al.* 2012) and published literature (Brown 2011 and references therein) for identification purposes.

HBI quantification

For gravimetric quantification of IP_{25}, GC–MS responses were obtained in selective ion monitoring (SIM) mode (*m/z* 350.3) and were normalised using instrumental response factors and the masses of internal standard and sample mass (Belt *et al.*, 2012).

iPOC quantification

Based on a previous method for estimating iPOC in seawater (Brown *et al.*, 2016), range and mean estimates of the iPOC content of amphipods ($iPOC_{amph}$) were obtained by combining amphipod IP_{25} concentrations with $iPOC/IP_{25}$ ratios derived from an ice algal aggregate sampled on 29 June 2012 (Eq. 1). $iPOC_{amph}$ concentration estimates were obtained for the five amphipod species sampled.

$$iPOC_{amph} = \mathrm{IP_{25\ (amphipod)}} \times \frac{\mathrm{iPOC\ (aggregate)}}{\mathrm{IP_{25\ (aggregate)}}} \quad (1)$$

HBI biomarker H-Print

H-Prints (%) were calculated using the abundance of pelagic (III) and sympagic (IP_{25} and II) HBIs according to Eq. 2.

$$\mathrm{H-Print\ \%} = \frac{(\mathrm{III})}{(\mathrm{IP_{25}} + \mathrm{II} + \mathrm{III})} \times 100 \quad (2)$$

In addition to quantifying sympagic carbon contribution to amphipod diet using equation 1, estimates of the proportion of sympagic carbon (with 99% confidence intervals), relative to total marine carbon (i.e. sympagic plus pelagic), were also derived by converting H-Prints using a previously modelled regression curve (Brown and Belt, 2017).

185

186 **Statistical analysis**

187 Statistical analysis was carried out in R-Studio version 1.0.136 (R-Core-Team, 2016).
188 ANOVA, with post-hoc Least Significant Difference mean separation tests (pairwise
189 comparisons), was used to compare $iPOC_{amph}$ between amphipod species. A student's t-test
190 for two samples was used to compare $iPOC_{amph}$ between different size groups of the same
191 species. All data are reported as mean ± standard error unless stated otherwise with tests
192 considered significant at $\alpha = 0.05$.

193

194 **RESULTS**

195 **Ice algae aggregates**

196 Taxonomic analysis of floating ice algal aggregates (1–15 cm in diameter) sampled within
197 the meltwater layer during the ICE12 cruise showed an assemblage of densely packed
198 diatoms, with a dominance of the ice-associated pennate diatoms *Navicula pelagica*,
199 *Hantzschia weyprechtii*, *Entomoneis paludosa* and *Cylindrotheca closterium* (Assmy *et al.*,
200 2013). Our analysis of one of these ice algal aggregates, which was sampled alongside
201 amphipods, showed a total organic carbon (TOC) content (261±5 mg g^{-1}; 26%) consistent
202 with previous data from diatom cultures (e.g. *Berkeleya rutilans* 30%; Brown *et al.*, 2014b)
203 and floating ice algal aggregates (27–31%; Brown *et al.*, 2014c). The IP_{25} content was
204 1.14±0.02 µg g^{-1}, giving an $iPOC/IP_{25}$ ratio of 2.29 ± 0.04 $\times 10^5$; $n = 6$. The dominance of sea
205 ice diatom species within the aggregate was also reflected in the H-Print (<1%; $n = 5$).

206

207 **iPOC in amphipods**

208 The mean abundance of the individual species, derived from 24 separate sampling operations
209 (Table 1, Fig. 3), showed that *Apherusa glacialis* (mean 7.7 ind. m^{-2}) and *Onisimus nanseni*

(0.1 ind. m^{-2}) were the most and least abundant species, respectively. The largest species, *Gammarus wilkitzkii*, was the second most abundant (0.7 ind. m^{-2}), while *Eusirus holmi* and *Onisimus glacialis* were comparable (0.3 ind. m^{-2}).

Our $iPOC_{amph}$ estimates show that *G. wilkitzkii* contained the most iPOC, with between 96 and 2052 µg C ind^{-1} for specimens ranging in length from 15–40 mm (Fig. 4a-b). Such specimens contained significantly more $iPOC_{amph}$ than any other species, including *E. holmi*, despite being of similar size (F = 15.8, df = 4, p = <0.001; Table 1). In general, larger individuals of *G. wilkitzkii* (>35 mm) had ca. 4 times more $iPOC_{amph}$ than smaller specimens (<20 mm) (t = 2.8, df = 9.3, p = 0.02). Normalisation of $iPOC_{amph}$ estimates to account for amphipod mass (dry) revealed that *O. glacialis* had the highest dry mass (DM) normalised $iPOC_{amph}$, with more than twice as much $iPOC_{amph}$ as any other species (F = 13.6, df = 4, p = <0.001; Table 1). In contrast to absolute $iPOC_{amph}$ estimates, the DM normalised $iPOC_{amph}$ content of *G. wilkitzkii* was similar to the much smaller *A. glacialis* (F = 13.6, df = 4, p = <0.001). Finally, DM normalised data revealed that *E. holmi* and *O. nanseni* had similar $iPOC_{amph}$ content, both being significantly less than other species (Table 1), despite their difference in size (28±1.5 mm and 14±4 mm respectively).

The quantity of $iPOC_{amph}$ per unit area of sea ice at the time of sampling was estimated by combining mean $iPOC_{amph}$ values with mean amphipod abundance derived from the 24 separate observations made during sampling. This showed that the amount of iPOC being retained by amphipods was ca. 0.66 mg iPOC m^{-2} (Table 1). The majority of $iPOC_{amph}$ was found within *G. wilkitzkii* (73%; 0.48 mg m^{-2}), followed by *A. glacialis* (19%), with *O. glacialis*, *E. holmi* and *O. nanseni* containing the least (all <5%; 0.03 mg m^{-2}). When compared to the carbon standing stock of ice algal aggregates (0.74 mg C m^{-2}; from Assmy *et al.* (2013)), $iPOC_{amph}$ in the five amphipod species corresponded to approximately 89% of available ice algal aggregate carbon.

235

236 **Source of amphipod POC**

237 The majority (95%) of amphipod H-Prints for all species ranged from 0.1 to 7.2% (Fig. 4g-h),
238 with only four individuals (all *A. glacialis*) having H-Prints >7.2% (12.0, 13.1, 40.1 and
239 62.2%). Using the regression model defined previously by Brown and Belt (2017), these H-
240 Print values were re-expressed to estimate % sympagic carbon consumed by amphipods. In
241 all cases, mean % sympagic consumption was estimated as >90% (Table 1).

242

243 **DISCUSSION**

244 **Organic carbon and IP_{25} content of sea ice algal aggregate**

245 The iPOC/IP_{25} ratio used in the current study ($2.29 \pm 0.04 \times 10^5$) is much higher than that
246 reported previously for sea ice POC from Resolute Bay in the Canadian Arctic (ca. 2.6×10^3;
247 Brown *et al*., 2016) and we provide two explanations for this. Firstly, in contrast to the
248 Resolute Bay sea ice samples, there were high amounts of extracellular polymeric substances
249 (EPS) in the ICE12 sea ice algal aggregates from the Arctic Ocean (Assmy *et al.*, 2013),
250 consistent with a ‘stressed/old’ community (Søreide *et al*., 2006), and supported further by
251 observations of a large number of empty diatom frustules (Assmy *et al*., 2013). In addition,
252 the percentage of IP_{25}-producing species in the ICE12 algae was lower (<0.1%) compared to
253 Resolute Bay (0.3–3.6%; Brown *et al*., 2014c). Since ICE12 aggregates were sampled from
254 within the water column, rather than directly from within sea ice, this reduction could
255 potentially be due to the *in-situ* incorporation of non-IP_{25} producing phytoplanktic species,
256 although Assmy *et al.* (2013) showed that the aggregate composition was dominated by ice-
257 associated diatoms and this is supported here by very low H-Prints (<1%). Instead, although
258 *Haslea crucigeroides*, a known producer of IP_{25} (Brown *et al.*, 2014c), could be identified in
259 the ICE12 aggregates (T. A. Brown, pers. obs.), it was not sufficiently abundant to be

included in previous taxonomical reports (Assmy *et al.*, 2013). Indeed, the IP_{25}-producing species (*H. crucigeroides, H. spicula, H. kjellmanii* and *Pleurosigma stuxbergii* var *rhomboides*) are typically <1% of sea ice diatom assemblages from north-east Svalbard and west Greenland (von Quillfeldt, 2000), while the same species comprised >3% of the diatoms present in the Resolute Bay aggregates (Brown *et al.*, 2014c and references therein). In any case, regardless of the exact reasons for the differences in $iPOC/IP_{25}$, this study reinforces the importance of measuring this ratio on a case-by-case basis, as recommended by Brown *et al.* (2016). In contrast, adoption of a fixed value for $iPOC/IP_{25}$ will likely lead to anomalous estimates of iPOC within suspended/sinking POC and food-web constituents, as discussed in detail by Brown *et al.* (2016).

Quantitative estimates of ice-derived organic carbon in amphipods

IP_{25} was present in each of the amphipod specimens analysed, enabling us to estimate $iPOC_{amph}$ in all cases. $iPOC_{amph}$ estimates varied by three orders of magnitude, broadly reflecting the range in amphipod size, with the smallest (*A. glacialis*) and largest (*G. wilkitzkii*) containing the lowest and highest $iPOC_{amph}$, respectively. Dry mass-normalised abundances showed the opposite trend, however, with smaller species (and smaller individuals of species) having relatively higher $iPOC_{amph}$, which aligns with smaller animals having to sustain higher weight-specific ingestion rates to offset their higher metabolic activity (c.f. larger animals) (Werner, 1997). On the other hand, this size-dependant difference in $iPOC_{amph}$ may potentially reflect the variable dietary preference of amphipods, especially as the smaller *A. glacialis* are more herbivorous than the larger and mainly omnivorous/carnivorous *G. wilkitzkii* (Poltermann, 2001).

Next, by expressing the $iPOC_{amph}$ values as a percentage of estimated amphipod carbon content (ca. 40%; Werner, 1997; Yuichiro and Tsutomu, 2003; Kiørboe, 2013; Fig

5e–f), our data show that <13% of amphipod body carbon comprised carbon derived from sea ice algal aggregates, in good agreement with data obtained from captive *G. wilkitzkii*, *O. nanseni* and *A. glacialis***,** which consumed between 0.1 and 16% of body carbon during experiments carried out in fixed-volume vessels containing physical ice substrate (Werner, 1997).

We then combined $iPOC_{amph}$ data with the TOC content of ICE12 aggregates to obtain estimates of the total mass of ice algae consumed by amphipods. Our data indicate that individual *G. wilkitzkii* had consumed between 0.5 and 5 mg of ice algal aggregate leading up to their capture during our sampling campaign. Since our data represent *in-situ* values, it is not possible to definitively report data as estimates of daily consumption rates that would facilitate direct comparisons with other studies. However, comparison of our $iPOC_{amph}$ estimates to consumption rates reported previously for *Gammarus* spp. feeding on macrophytes in the Baltic Sea (1–5 mg ind. d^{-1}; Orav-Kotta *et al.*, 2009) and captive *G. wilkitzkii* (0.08–0.14 mg algae ind. d^{-1}; Werner, 1997), indicate that our estimates likely also reflect grazing rates over approximately 24 h. Further direct comparisons of $iPOC/IP_{25}$ derived values between *in-situ* and captive zooplankters might improve such comparisons in the future.

Finally, by combining $iPOC_{amph}$ with amphipod abundance (i.e. number of individuals per unit area) for each of the five species, we estimate that $iPOC_{amph}$ accounted for ca. 89% of the available ice algal aggregate carbon during the course of sampling, which agrees well with previous estimates of 63% and 58–92% (Siferd *et al.*, 1997; Kohlbach *et al.*, 2016). Similarly, our consistent amphipod H-Prints indicate that most amphipod species appeared to be obtaining energy almost exclusively (>90%; Table 1) from ice algal aggregates. On the other hand, based on a composite of field-measured abundances and laboratory-based grazing studies, Werner (1997) estimated the daily grazing impacts of *A. glacialis*, *Onisimus* spp. and

G. wilkitzkii to be ca. 1.1 and 2.6% for the Laptev and Greenland Sea, respectively. One explanation for these different outcomes might be associated with the high degree of variability in amphipod abundance, which is strongly seasonally dependent in response to the development of sea ice (Siferd *et al.*, 1997; Werner and Auel, 2005). Thus, it is possible that our amphipod abundances (and therefore estimates of grazing impact) were influenced, to some extent, by the sea ice conditions during the late melt season, when the sea ice was becoming increasingly heterogeneous, with a growing number of melt ponds (Assmy *et al.*, 2013). At this time in the season, after much of the iPOC had likely already been exported (e.g. Brown *et al.*, 2016), it is also possible that ice algae aggregates represented an important and concentrated food source in an otherwise relatively oligotrophic period. In this case, amphipod diet at the time of sampling would likely be dominated by ice algae, rather than other sources, resulting in relatively high estimates of grazing impact.

A part of $iPOC_{amph}$ could have been acquired from other carbon sources since, for example, large *G. wilkitzkii* has an omnivorous diet, and consumes both zooplankton and ice amphipods (Werner, 1997; Søreide *et al.*, 2006). The most likely candidates of zooplankton prey is *Calanus glacialis*, which is known to utilize ice algal blooms to fuel early maturation and reproduction (Søreide *et al.*, 2010). Qualitative assessment of herbivory/carnivory in amphipods has been established based on faecal pellet colouration, where green-yellow and orange-red pigments indicate herbivory and carnivory, respectively (Werner, 2000). Accordingly, the observed orange colouration of *G. wilkitzkii* lipid extracts in this study likely indicates that this species incorporated at least some of the estimated $iPOC_{amph}$ through carnivory, likely from *Calanus* sp., rather than direct herbivory. Despite this, we note that our *G. wilkitzkii* $iPOC_{amph}$ data remain comparable to other captive grazing experiments where carnivory was absent (Fig. 4 d,f; Werner, 1997). Indeed, it is well established that IP_{25} is transferred across trophic levels, and is readily identified in Arctic consumers, from fish

(Brown and Belt, 2012b; Brown *et al.*, 2015) and seabirds (Megson *et al.*, 2014), right up to marine mammals (Brown *et al.*, 2013, 2014a).

iPOC$_{amph}$ in *Eusirus holmi*

In contrast to the other amphipod species in this study, comparison of iPOC$_{amph}$ data with literature values was not possible for *E. holmi*, despite this species being pan-Arctic in distribution (Tencati and Geiger, 1968; Siferd, 2015). The limited reporting of *E. holmi* likely reflects its low abundance in the Arctic, rather than difficulties in identification, as it is easily recognized based on its light orange eyes, orange markings on coxa and pleopods, and four long antennae and long leg segments. *Eusirus holmi* accounted for ca. 3% of the amphipods in our samples and was even lower (<1%) in a previous study from the same region (Macnaughton *et al.*, 2007). Our iPOC$_{amph}$ data therefore likely represent the only documented estimates of iPOC consumption for this species. Notably, absolute iPOC$_{amph}$ estimates in *E. holmi* were most similar to those for the smaller *A. glacialis* and *O. nanseni*, while normalised (dry body mass) values were also comparable to the much smaller *O. nanseni*. Although the paucity of literature data prevents us from assessing our iPOC$_{amph}$ estimate for *E. holmi* further, we note that, in contrast to the other species investigated here, a relatively low iPOC$_{amph}$ content for this species might imply that it obtained the majority of its organic carbon from sources other than sea ice algae. *Eusirus holmi* is frequently observed by divers in the water column, typically with legs spread out to suspend itself while slowly sinking. It occasionally propels itself upwards with its large telson and then repeats the slow sinking. This likely represents the feeding behaviour of *E. holmi* in the water column, but it can also be observed clinging to the underside of sea ice. However, the consistent H-Print values indicated that ca. 100% (86-115%; 99% CI) of marine carbon in amphipods was of sympagic origin (Table 1). While there are a number of potential reasons for the low

360 $iPOC_{amph}$ estimates, including, for example, selectivity during grazing, further analysis of this
361 species will be necessary before firmer conclusions can be made. What is clear, however, is
362 that the low field abundances of *E. holmi* in other studies and low $iPOC_{amph}$ content estimated
363 here indicate that this species is currently of minor importance with respect to channelling the
364 sympagic carbon component into the ecosystem, at least in comparison to other more
365 abundant species in this study, particularly, *G. wilkitzkii* and *A. glacialis*.
366
367 Having focused here on a somewhat localised setting, we anticipate that further application of
368 this technique to a wider range of Arctic ice fauna and zooplankters has the potential to
369 improve our knowledge and understanding of the role that ice algae play in supporting the
370 broader Arctic ecosystem. Concomitant with the long-term trend of decreasing sea ice extent
371 and thickness (Barber *et al.*, 2015), a similar decline in ice-amphipods, particularly *G.*
372 *wilkitzkii* has occurred, with associated reduction of high-energy food to upper trophic
373 consumers (Hop *et al.*, 2013). Reduction in sea ice extent in Antarctica has similarly been
374 identified as one of the causes of the recent decline in Antarctic krill populations in the
375 Southern Ocean (Flores *et al.*, 2012), with impacts on higher trophic level animals (Reiss *et*
376 *al.*, 2017). In both polar areas, increased ridging in thinner ice may partly compensate for loss
377 in sea ice extent by creating complex structures as enhanced habitat for sympagic fauna
378 (Gradinger et al., 2010; Melbourne-Thomas et al., 2016). The more pelagic *E. holmi* may
379 increase in abundance with changing ice conditions towards thinner first-year ice and more
380 frequent open water in the Arctic Ocean. Under such a scenario, *E. holmi* may potentially
381 represent an alternative energy source to that currently derived from ice algae (and associated
382 amphipods) and, therefore, an important target for future research efforts. In any case, the
383 data generated from this, and subsequent studies, will provide the necessary numerical input
384 required to assist models in predicting the potential impact of declining Arctic sea ice extent

on sea ice biota, and further evaluation of sea ice algae as an energy source for other Arctic consumers.

CONCLUSION

Our data provide evidence to support our initial hypothesis that combining sea ice-derived iPOC/IP_{25} data with IP_{25} concentration data obtained from amphipods can provide realistic estimates of the amount of sympagic organic carbon within these primary consumers. Accordingly, we present quantitative estimates of iPOC for ice-associated amphipods and the first documented assessment of the sympagic carbon content of the understudied *E. holmi*. Our findings are also supported by data obtained from the same samples using a combined biomarker approach (H-Print). The data generated from this, and subsequent studies, will provide numerical input required to assist models in predicting the potential impact of declining Arctic sea ice extent on sea ice biota, and to further evaluate sea ice algae as an energy source for other Arctic consumers.

403 ACKNOWLEDGEMENTS

404 We are indebted to the captain and crew of RV *Lance*. We are also grateful to A Tonkin
405 (University of Plymouth) for carrying out CHN analysis of algal aggregates. Taxonomic
406 analyses were based on a contract with Institute of Oceanology, Sopot, Poland, with expertise
407 administered by Slawomir Kwasniewski. We are also grateful to the Associate Editor and an
408 anonymous reviewer for their helpful comments.

409

410 FUNDING

411 This work was supported by the award of a Research Project Grant from the Leverhulme
412 Trust (UK). The ICE2012 cruise was funded and conducted as part of the Centre for Ice,
413 Climate and Ecosystems (ICE) at the Norwegian Polar Institute.

414

415

Table 1. Mean (± se) and relative (%) amphipod abundance, ice-derived particulate organic carbon ($iPOC_{amph}$) and H-Print estimates (99% CI) of sympagic carbon, as a percentage of sympagic and pelagic marine carbon consumed, based on the regression model of Brown and Belt (2017).

	Abundance			$iPOC_{amph}$										H-Print estimates (%) of sympagic carbon			
Species	*n*	ind. m^{-2}	% of all species	*n*	µg C ind^{-1}	% of all species	Significant difference[1]	mg C g^{-1} DM	% of all species	Significant difference[1]	iPOC % amphipod C	Significant difference[1]	mg C m^{-2}	% of all species	Mean (99% CI)	Max (99% CI)	Min (99% CI)	Significant difference[1]
Apherusa glacialis	*367*	7.7	85	*15*	16.3 ± 2.4	2	a	9.8 ± 1.9	21	a	2.5 ± 0.5	a	0.13	19	92 (78-106)	100 (86-115)	37 (24-52)	a
Eusirus holmi	*12*	0.3	3	*14*	54.7 ± 8.3	6	a	1.6 ± 0.2	3	b	0.4 ± 0.1	b	0.01	2	100 (86-115)	100 (86-115)	100 (86-115)	b
Onisimus nansenii	*6*	0.1	1	*13*	68.5 ± 18.9	7	a	5.1 ± 1.1	11	ab	1.3 ± 0.3	ab	0.01	1	100 (86-115)	100 (86-115)	99 (84-113)	b
Onisimus glacialis	*15*	0.3	3	*10*	107.5 ± 14.5	12	a	23.5 ± 4.5	49	c	5.9 ± 1.1	c	0.03	5	100 (86-115)	100 (86-115)	100 (86-115)	b
Gammarus wilkitzkii	*34*	0.7	8	*34*	673.6 ± 94.5	73	b	7.8 ± 1.3	16	a	2.0 ± 0.3	a	0.48	73	99 (84-113)	100 (86-115)	93 (79-108)	b

Total	*434*	9.14*	*86*	920.6*	47.8*	0.66*

419 * Calculated from mean values

420 [1] Least Significant Difference mean separation tests (pairwise comparisons), $\alpha = 0.05$

421 REFERENCES

422 Arndt, C. E. and Swadling, K. M. (2006) Crustacea in Arctic and Antarctic Sea Ice:
423 Distribution, diet and life history strategies. *Adv. Mar. Biol.* **51**, 197-315.
424 Arrigo, K. R. (2014) Sea ice ecosystems. *Ann. Rev. Mar. Sci.*, **6,** 439-467.
425 Assmy, P., Ehn, J. K., Fernández-Méndez, M., Hop, H., Katlein, C., Sundfjord, A., Bluhm,
426 K., Daase, M., Engel, A., Fransson, A., Granskog, M. A., Hudson, S. R., Kristiansen,
427 S., Nicolaus, M., Peeken, I., Renner, A. H. H., Spreen, G., Tatarek, A. and Wiktor, J.
428 (2013) Floating ice-algal aggregates below melting Arctic sea ice. *PLoS ONE,* **8,**
429 e76599.
430 Barber, D. G., Hop, H., Mundy, C. J., Else, B., Dmitrenko, I. A., Tremblay, J.-E., Ehn, J. K.,
431 Assmy, P., Daase, M., Candlish, L. M. and Rysgaard, S. (2015) Selected physical,
432 biological and biogeochemical implications of a rapidly changing Arctic Marginal Ice
433 Zone. *Progr. Oceanogr.*, **139,** 122-150.
434 Belt, S. T., Brown, T. A., Navarro-Rodriguez, A., Cabedo-Sanz, P., Tonkin, A. and Ingle, R.
435 (2012) A reproducible method for the extraction, identification and quantification of
436 the Arctic sea ice proxy IP_{25} from marine sediments. *Anal. Methods,* **4,** 705-713.
437 Belt, S. T., Massé, G., Rowland, S. J., Poulin, M., Michel, C. and Leblanc, B. (2007) A novel
438 chemical fossil of palaeo sea ice: IP_{25}. *Org. Geochem.*, **38,** 16-27.
439 Belt, S. T., Massé, G., Vare, L. L., Rowland, S. J., Poulin, M., Sicre, M.-A., Sampei, M. and
440 Fortier, L. (2008) Distinctive ^{13}C isotopic signature distinguishes a novel sea ice
441 biomarker in Arctic sediments and sediment traps. *Mar. Chem.*, **112,** 158-167.
442 Belt, S. T. and Müller, J. (2013) The Arctic sea ice biomarker IP_{25}: a review of current
443 understanding, recommendations for future research and applications in palaeo sea ice
444 reconstructions. *Quat. Sci. Rev.*, **79,** 9-25.

Brown, T. A. (2011) *Production and preservation of the Arctic sea ice diatom biomarker IP_{25}. PhD Thesis.* University of Plymouth.

Brown, T. A., Alexander, C., Yurkowski, D. J., Ferguson, S. and Belt, S. T. (2014a) Identifying variable sea ice carbon contributions to the Arctic ecosystem: A case study using highly branched isoprenoid lipid biomarkers in Cumberland Sound ringed seals. *Limnol. Oceanogr.,* **59,** 1581-1589.

Brown, T. A. and Belt, S. T. (2012a) Closely linked sea ice–pelagic coupling in the Amundsen Gulf revealed by the sea ice diatom biomarker IP_{25}. *J. Plankton Res.,* **34,** 647-654.

Brown, T. A. and Belt, S. T. (2012b) Identification of the sea ice diatom biomarker IP_{25} in Arctic benthic macrofauna: Direct evidence for a sea ice diatom diet in Arctic heterotrophs. *Polar Biol.,* **35,** 131-137.

Brown, T. A. and Belt, S. T. (2017) Biomarker-based H-Print quantifies the composition of mixed sympagic and pelagic algae consumed by *Artemia* sp. *J. Exp. Mar. Biol. Ecol.,* **488,** 32-37.

Brown, T. A., Chrystal, E., Ferguson, S. H., Yurkowski, D. J., Watt, C., Hussey, N. and Belt S. T. (2017) Coupled changes in the sea ice carbon contribution to diet and trophic position of Cumberland Sound beluga whales identified by H-Print and $\delta^{15}N$ analysis. *Limnol. Oceanogr*. (In press).

Brown, T. A., Belt, S. T. and Cabedo-Sanz, P. (2014b) Identification of a novel di-unsaturated C_{25} highly branched isoprenoid in the marine tube-dwelling diatom *Berkeleya rutilans*. *Environ. Chem. Lett.*, **12,** 455-460.

Brown, T. A., Belt, S. T., Ferguson, S. H., Yurkowski, D. J., Davison, N. J., Barnett, J. E. F. and Jepson, P. D. (2013) Identification of the sea ice diatom biomarker IP_{25} and related lipids in marine mammals: A potential method for investigating regional

variations in dietary sources within higher trophic level marine systems. *J. Exp. Mar. Biol. Ecol.*, **441,** 99-104.

Brown, T. A., Belt, S. T., Gosselin, M., Levasseur, M., Poulin, M. and Mundy, C. J. (2016) Quantitative estimates of sinking sea ice particulate organic carbon based on the biomarker IP_{25}. *Mar. Ecol. Prog. Ser.*, **546,** 17-29.

Brown, T. A., Belt, S. T., Philippe, B., Mundy, C. J., Massé, G., Poulin, M. and Gosselin, M. (2011) Temporal and vertical variations of lipid biomarkers during a bottom ice diatom bloom in the Canadian Beaufort Sea: Further evidence for the use of the IP_{25} biomarker as a proxy for spring Arctic sea ice. *Polar Biol.*, **34,** 1857-1868.

Brown, T. A., Belt, S. T., Tatarek, A. and Mundy, C. J. (2014c) Source identification of the Arctic sea ice proxy IP_{25}. *Nat. Comms.*, **5**, 4197.

Brown, T. A., Hegseth, E. N. and Belt, S. T. (2015) A biomarker-based investigation of the mid-winter ecosystem in Rijpfjorden, Svalbard. *Polar Biol.*, **38,** 37-50.

Brown, T. A., Yurkowski, D. J., Ferguson, S. H., Alexander, C. and Belt, S. T. (2014d) H-Print: a new chemical fingerprinting approach for distinguishing primary production sources in Arctic ecosystems. *Environ. Chem. Lett.*, **12,** 387-392.

Dalpadado, P., Hop, H., Rønning, J., Pavlov, V., Sperfeld, E., Buchholz, F., Rey A, Wold, A. (2016) Distribution and abundance of euphausiids and pelagic amphipods in Kongsfjorden, Isfjorden and Rijpfjorden (Svalbard) and changes in their relative importance as key prey in a warming marine ecosystem. *Polar Biol.*, **39**, 1765-1784.

Dieckmann, G. S. and Hellmer, H. H. (2010) The importance of sea ice: An overview. In: D. Thomas and S. Dieckmann (eds) *Sea ice (second edition).* Blackwell Publishing, Chichester, pp. 1-22.

Flores, H., Atkinson, A., Kawaguchi, S., Krafft, B. A., Milinevsky, G., Nicol, S., Reiss, C., Tarling, G. A., Werner, R., Rebolledo, E. B., Cirelli, V., Cuzin-Roudy, J., Fielding,

S., Groeneveld, J. J., Haraldsson, M., Lombana, A., Marschoff, E., Meyer, B., Pakhomov, E. A., Rombola, E., Schmidt, K., Siegel, V., Teschke, M., Tonkes, H., Toullec, J. Y., Trathan, P. N., Tremblay, N., Van De Putte, A. P., Van Franeker, J. A. and Werner, T. (2012) Impact of climate change on Antarctic krill. *Mar. Ecol. Prog. Ser.*, **458,** 1-19.

Gradinger, R., Bluhm, B. and Iken, K. (2010) Arctic sea-ice ridges--Safe heavens for sea-ice fauna during periods of extreme ice melt? *Deep-Sea Res. II*, **57**, 86-95

Hop, H., Bluhm, B. A., Daase, M., Gradinger, R., Poulin, M. (2013) Arctic Sea Ice Biota. Arctic Report Cards, NOAA. <http://www.arctic.noaa.gov/reportcard>.

Hop, H., Poltermann, M., Lønne, O. J., Falk-Petersen, S., Korsnes, R., Budgell, W. P. (2000) Ice amphipod distribution relative to ice density and under-ice topography in the northern Barents Sea. *Polar Biol.*, **23**, 367-367.

Jakobsson, M., Mayer, L., Coakley, B., Dowdeswell, J. A., Forbes, S., Fridman, B., Hodnesdal, H., Noormets, R., Pedersen, R., Rebesco, M., Schenke, H. W., Zarayskaya, Y., Accettella, D., Armstrong, A., Anderson, R. M., Bienhoff, P., Camerlenghi, A., Church, I., Edwards, M., Gardner, J. V., Hall, J. K., Hell, B., Hestvik, O., Kristoffersen, Y., Marcussen, C., Mohammad, R., Mosher, D., Nghiem, S. V., Pedrosa, M. T., Travaglini, P. G. and Weatherall, P. (2012) The International Bathymetric Chart of the Arctic Ocean (IBCAO) Version 3.0. *Geophys. Res. Lett.*, **39**, L12609.

Kiørboe, T. (2013) Zooplankton body composition. *Limnol. Oceanogr.*, **58,** 1843-1850.

Kohlbach, D., Graeve, M., Lange, B., David, C., Peeken, I. and Flores, H. (2016) The importance of ice algae-produced carbon in the central Arctic Ocean ecosystem: Food web relationships revealed by lipid and stable isotope analyses *Limnol. Oceanogr.*, **61,** 2027-2044..

520 Kraft, A., Bauerfeind, E. and Nöthig, E.-M. (2010) Amphipod abundance in sediment trap
521 samples at the long-term observatory HAUSGARTEN (Fram Strait, ~79°N/4°E).
522 Variability in species community patterns. *Mar. Biodivers.,* **41,** 353-364.
523 Leu, E., Mundy, C. J., Assmy, P., Campbell, K., Gabrielsen, T. M., Gosselin, M., Juul-
524 Pedersen, T. and Gradinger, R. (2015) Arctic spring awakening – Steering principles
525 behind the phenology of vernal ice algal blooms. *Progr. Oceanogr.,* **139:** 151-170
526 Lønne, O. J. (1988) A diver-operated electric suction sampler for sympagic (=under-ice)
527 invertebrates. *Polar Res.*, **6**, 135-136.
528 Lønne, O. J., Gabrielsen, G. W. (1992) Summer diet of seabirds feeding in sea-ice-covered
529 waters near Svalbard. *Polar Biol.*, **12**, 685-692.
530 Lønne, O. J. and Gulliksen, B. (1989) Size, age and diet of polar cod, *Boreogadus saida*
531 (Lepechin 1773), in ice covered waters. *Polar Biol.,* **9,** 187-191.
532 Macnaughton, M., Thormar, J. and Berge, J. (2007) Sympagic amphipods in the Arctic pack
533 ice: redescriptions of *Eusirus holmii* Hansen, 1887 and *Pleusymtes karstensi* Barnard,
534 1959. *Polar Biol.,* **30,** 1013-1025.
535 Megson, D., Brown, T. A., Johnson, G. W., O’Sullivan, G., Bicknell, A. W. J., Votier, S. C.,
536 Lohan, M. C., Comber, S., Kalin, R. and Worsfold, P. J. (2014) Identifying the
537 provenance of Leach’s storm petrels in the North Atlantic using polychlorinated
538 biphenyl signatures derived from comprehensive two-dimensional gas
539 chromatography with time-of-flight mass spectrometry. *Chemosphere,* **114,** 195-202.
540 Melbourne-Thomas, J., Corney, S. P., Trebilco, R., Meiners, K. M., Stevens, R. P.,
541 Kawaguchi, S., Sumner, M. D. and Constable, A. J. (2016) Under ice habitats for
542 Antarctic krill larvae: Could less mean more under climate warming? *Geophys. Res.*
543 *Lett.*, **43**, 10322-10327.

Nygård, H., Vihtakari, M. and Berge, J. (2009) Life history of *Onisimus caricus* (Amphipoda: Lysianassoidea) in a high Arctic fjord. *Aquat. Biol.,* **5**, 63-74.

Orav-Kotta, H., Kotta, J., Herkül, K., Kotta, I. and Paalme, T. (2009) Seasonal variability in the grazing potential of the invasive amphipod *Gammarus tigrinus* and the native amphipod *Gammarus salinus* (Amphipoda: Crustacea) in the northern Baltic Sea. *Biol. Invasions,* **11,** 597-608.

Poltermann, M. (2001) Arctic sea ice as feeding ground for amphipods – food sources and strategies. *Polar Biol.,* **24,** 89-96.

R-Core-Team (2016) R: A language and environment for statistical computing. *R Foundation for Statistical Computing, Vienna, Austria.* pp. URL http://www.R-project.org/.

Reiss, C. S., Cossio, A., Santora, J. A., Dietrich, K. S., Murray, A., Mitchell, B. G., Walsh, J., Weiss, E. L., Gimpel, C., Jones, C. D. and Watters, G. M. (2017) Overwinter habitat selection by Antarctic krill under varying sea-ice conditions: implications for top predators and fishery management. *Mar. Ecol. Prog. Ser.*, **568,** 1-16.

Serreze, M. C., Crawford, A. D., Stroeve, J. C., Barrett, A. P. and Woodgate, R. A. (2016) Variability, trends, and predictability of seasonal sea ice retreat and advance in the Chukchi Sea. *J. Geophys. Res. Ocean.,* **121,** 7308-7325.

Siferd, T. D. (2015) Central and Arctic Multi-Species Stock Assessment Surveys Version 5 In OBIS Canada Digital Collections. Bedford Institute of Oceanography, Dartmouth, NS, Canada. Published by OBIS, Digital http://www.iobis.org/. Accessed on 15-12-2016.

Siferd, T. D., Welch, H. E., Bergmann, M. A. and Curtis, M. F. (1997) Seasonal distribution of sympagic amphipods near Chesterfield Inlet, N.W.T., Canada. *Polar Biol.,* **18,** 16-22.

568 Søreide, J. E., Carroll, M. L., Hop, H., Ambrose Jr., W. G., Hegseth, E. N., and Falk-
569 Petersen, S. (2013) Sympagic-pelagic-benthic coupling in Arctic and Atlantic waters
570 around Svalbard revealed by stable isotopic and fatty acid tracers. *Mar. Biol. Res.*, **9**,
571 831-850.
572 Søreide, J. E., Hop, H., Carroll, M. L., Falk-Petersen, S. and Hegseth, E. N. (2006) Seasonal
573 food web structures and sympagic–pelagic coupling in the European Arctic revealed
574 by stable isotopes and a two-source food web model. *Progr. Oceanogr.*, **71,** 59-87.
575 Søreide, J. E., Leu, E., Berge, J., Graeve, M. and Falk-Petersen, S. (2010) Timining in
576 blooms, algal food quality and *Calanus glacialis* reproduction and growth in a
577 changing Arctic. *Glob. Change Biol.*, **16**, 3154-3163.
578 Tencati, J. R. and Geiger, S. R. (1968) Pelagic amphipods of the slope waters of Northeast
579 Greenland. *J. Fish. Res. Board Can.*, **25,** 1637-1650.
580 von Quillfeldt, C. H. (2000) Common diatom species in Arctic spring blooms: their
581 distribution and abundance. *Bot. Mar.*, **43**, 499-516.
582 Werner, I. (1997) Grazing of Arctic under-ice amphipods on sea-ice algae. *Mar. Ecol. Prog.*
583 *Ser.*, **160,** 93-99.
584 Werner, I. (2000) Faecal pellet production by Arctic under-ice amphipods – transfer of
585 organic matter through the ice/water interface. *Hydrobiologia*, **426,** 89-96.
586 Werner, I. and Auel, H. (2005) Seasonal variability in abundance, respiration and lipid
587 composition of Arctic under-ice amphipods. *Mar. Ecol. Prog. Ser.*, **292,** 251-262.
588 Yuichiro, Y. and Tsutomu, I. (2003) Metabolism and chemical composition of four pelagic
589 amphipods in the Oyashio region, western subarctic Pacific Ocean. *Mar. Ecol. Prog.*
590 *Ser.*, **253,** 233-241.

591

592

593 Figure captions

594

595 Fig. 1 Structures of sea ice diatom (IP_{25}, II) and phytoplanktic diatom (III) highly branched
596 isoprenoids (HBIs) measured in amphipods.

597

598 Fig. 2 Study location north of Svalbard with bathymetry. Green line is the drift trajectory of
599 the ice floe that the RV *Lance* was moored to, with start and end dates. The ice edge positions
600 for 27, 31 July and 2 August are indicated by the broken lines and are representative for the
601 drift period. Map created by the Norwegian Polar Institute, Max König. Bathymetry with
602 permission from IBACO (Jakobsson *et al.*, 2012).

603

604 Fig. 3 Averaged amphipod abundance for each species beneath the ice floe during sampling
605 (note: logged y-axis). Circles = flat under-ice surface, squares = ridged under-ice surface.

606

607 Fig. 4 Amphipod iPOC content (a-f) and H-Print (g-h; note logged scale) compared to
608 amphipod length (left) and for species average (right). Horizontal dotted lines (a, b) represent
609 equivalent total algal aggregate mass consumed for selected iPOC concentrations (note
610 logged scale in b). Red dots (d and f) show data derived from laboratory experiments
611 (Werner, 1997). Green dots (h) show the H-Print value derived from ice algal aggregates that
612 amphipods were observed grazing upon in this study.

613

614

615

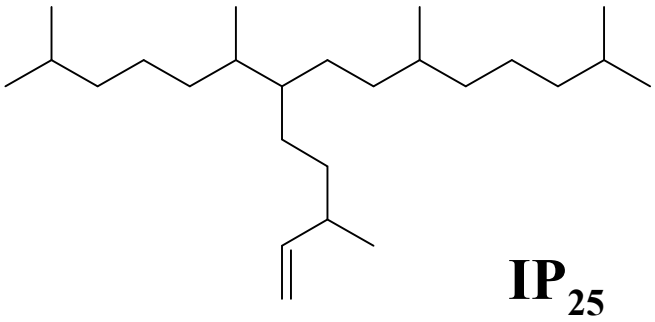

IP_{25}

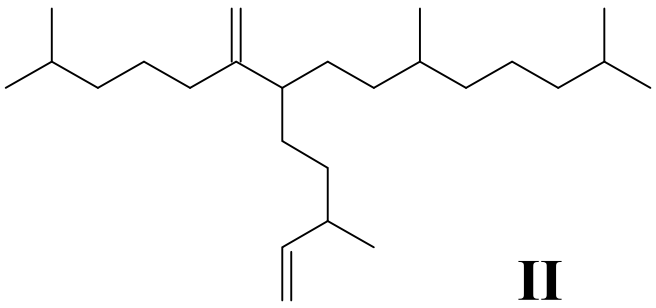

II

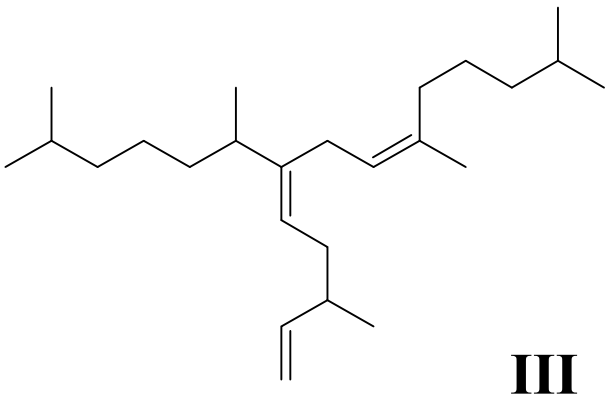

III

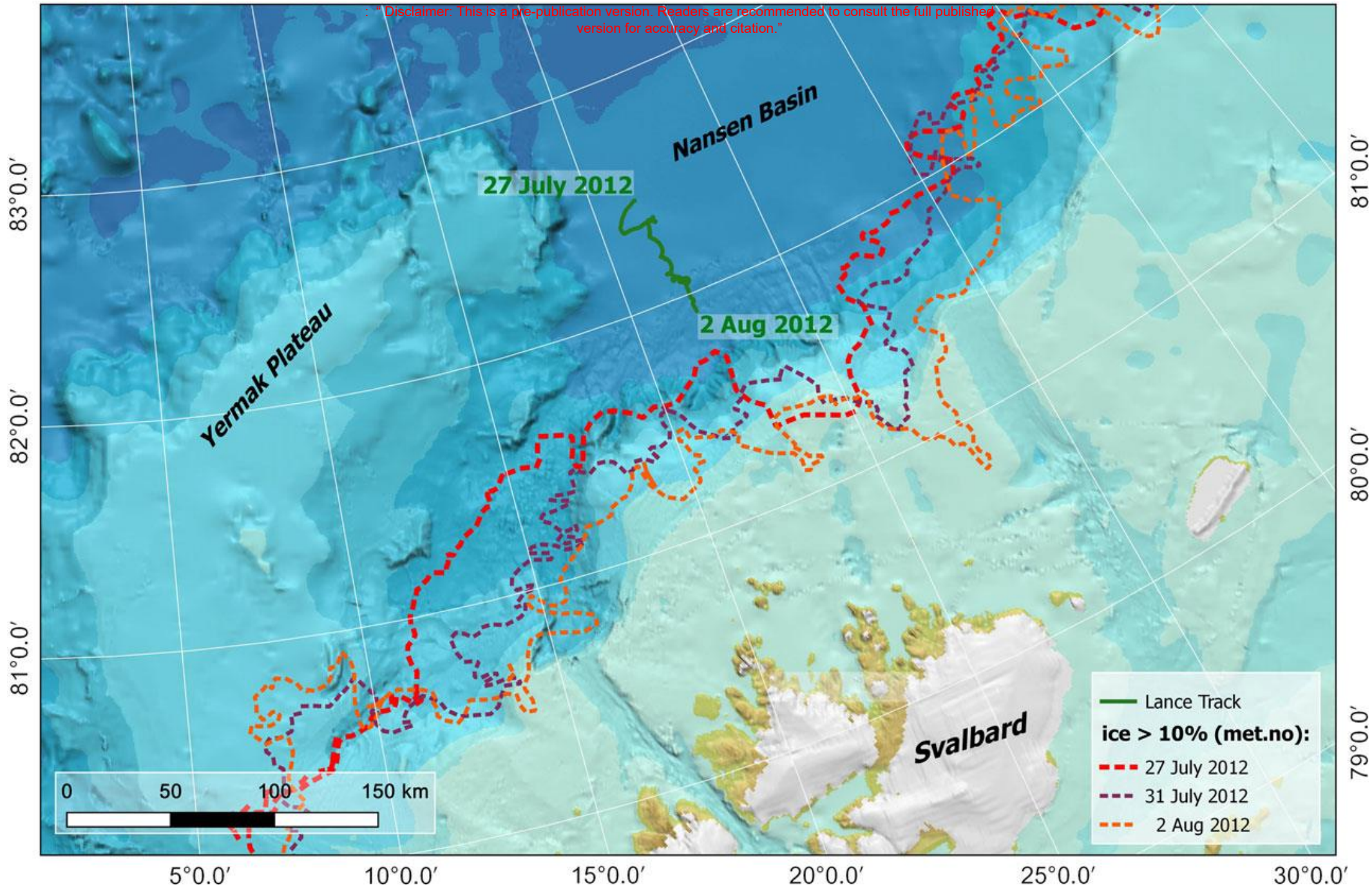

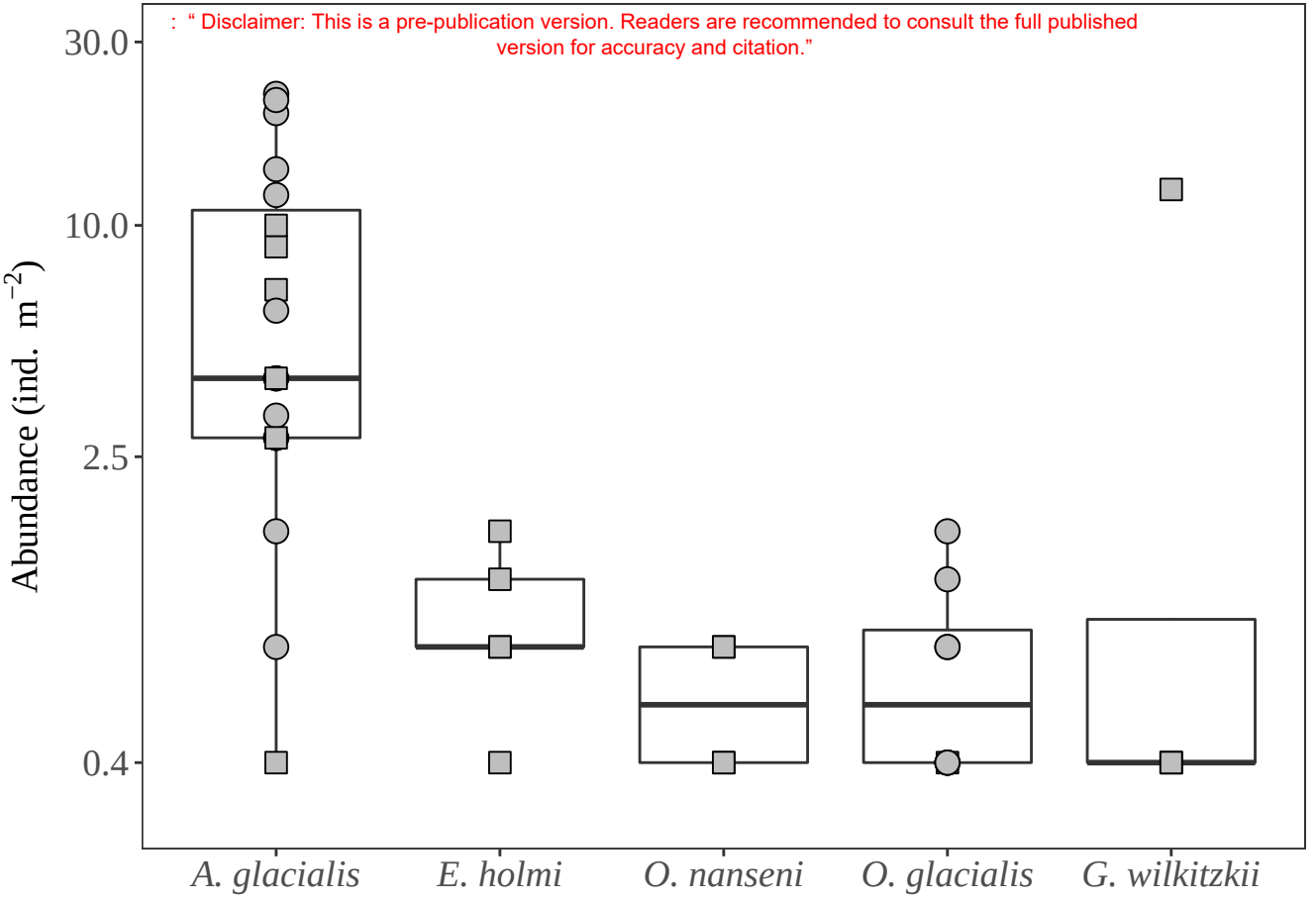

a

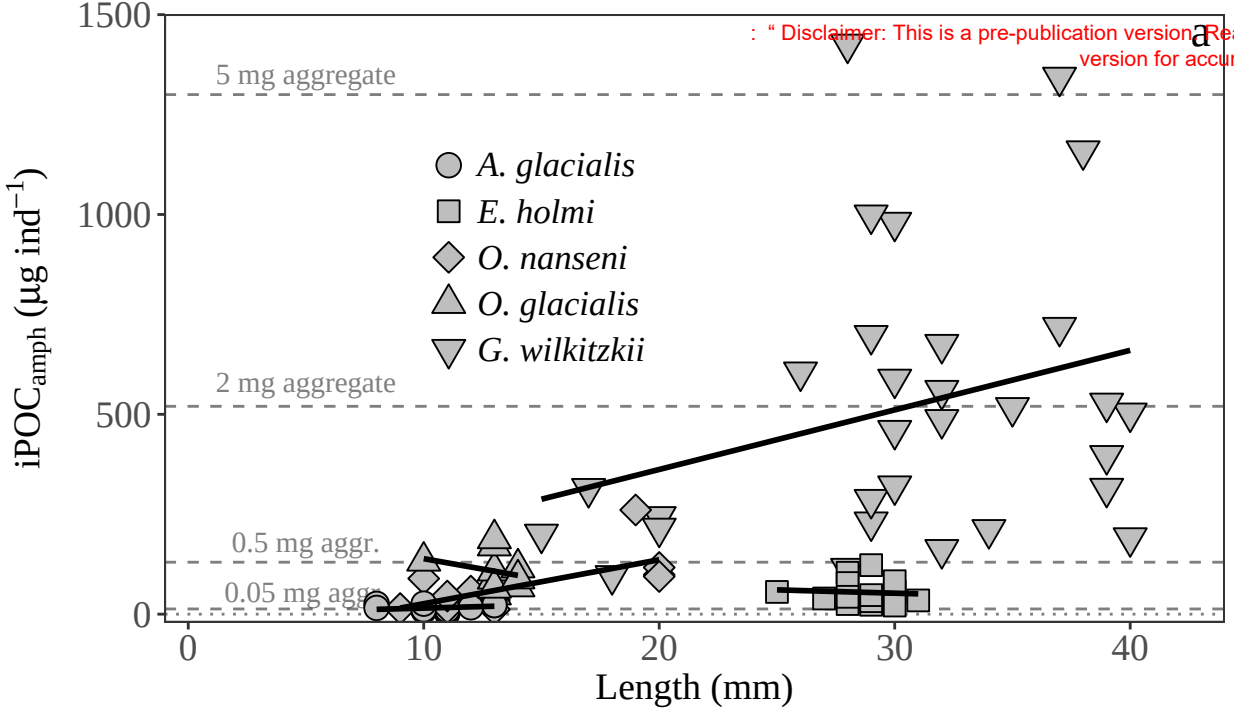

b

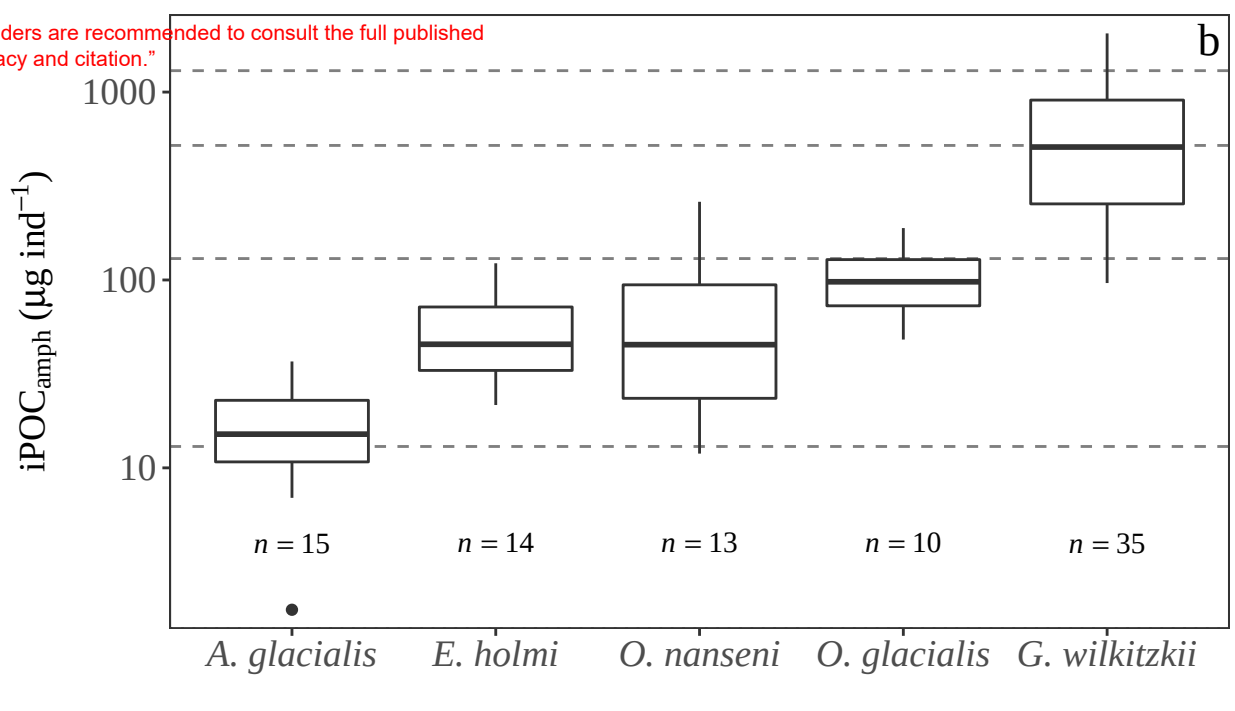

c

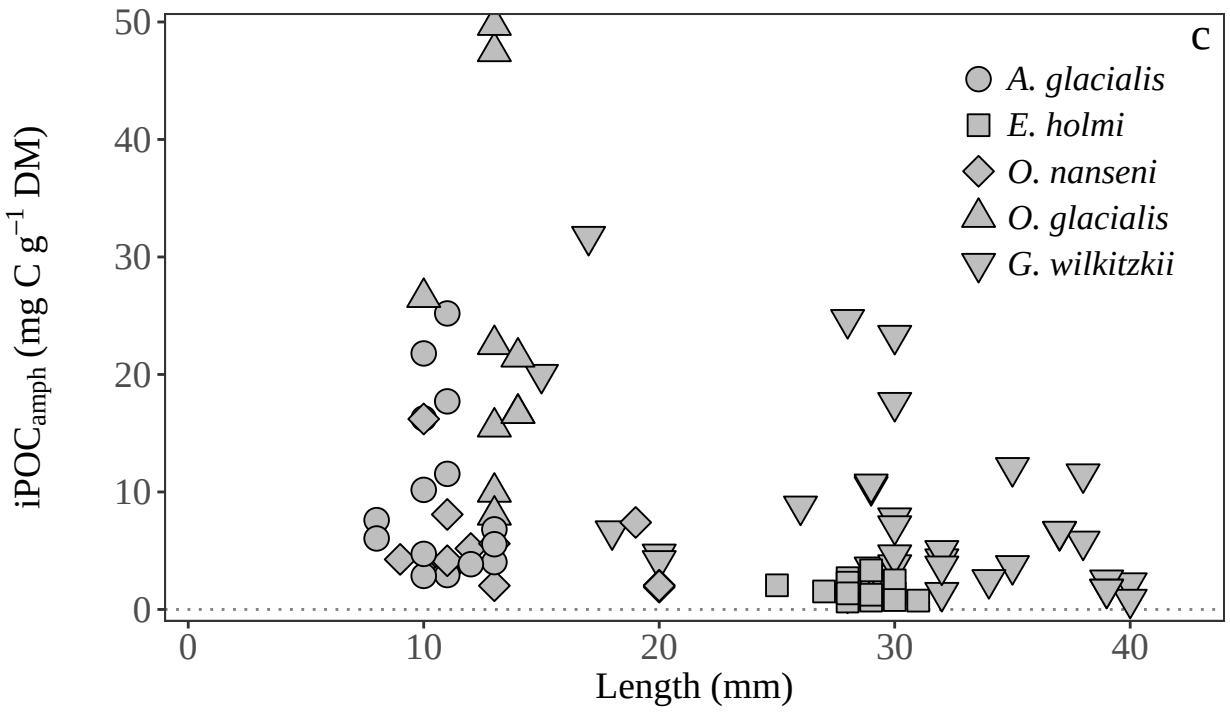

d

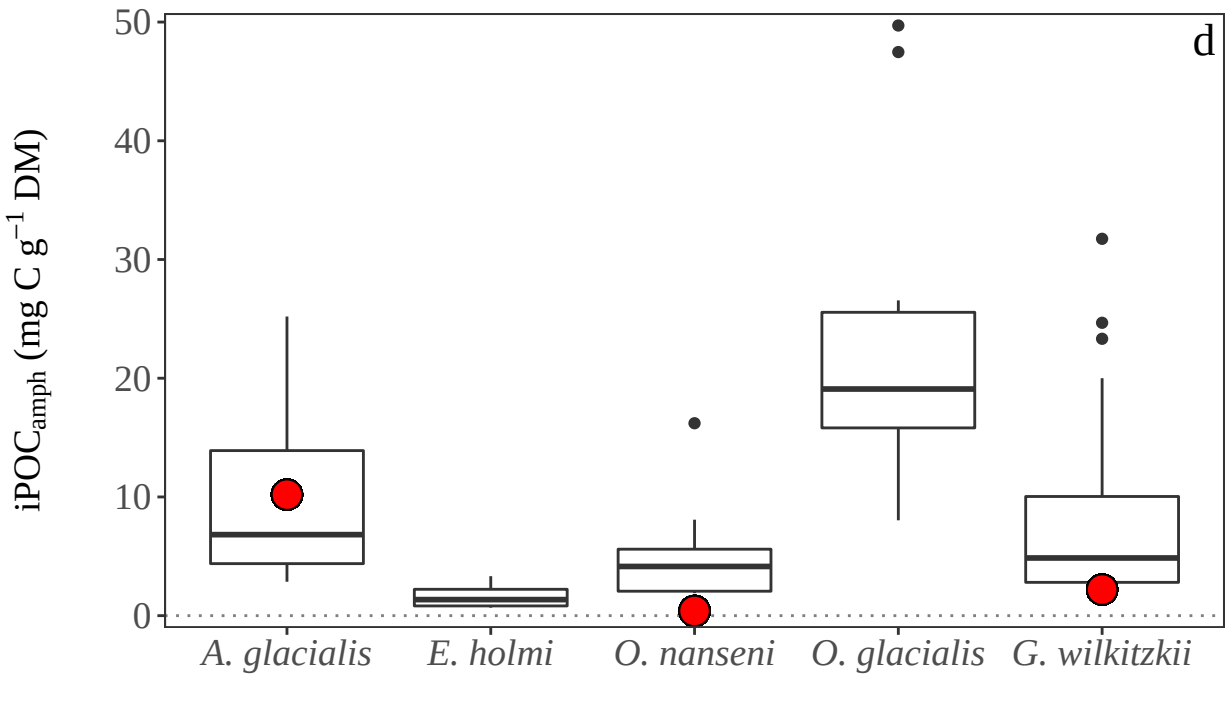

e

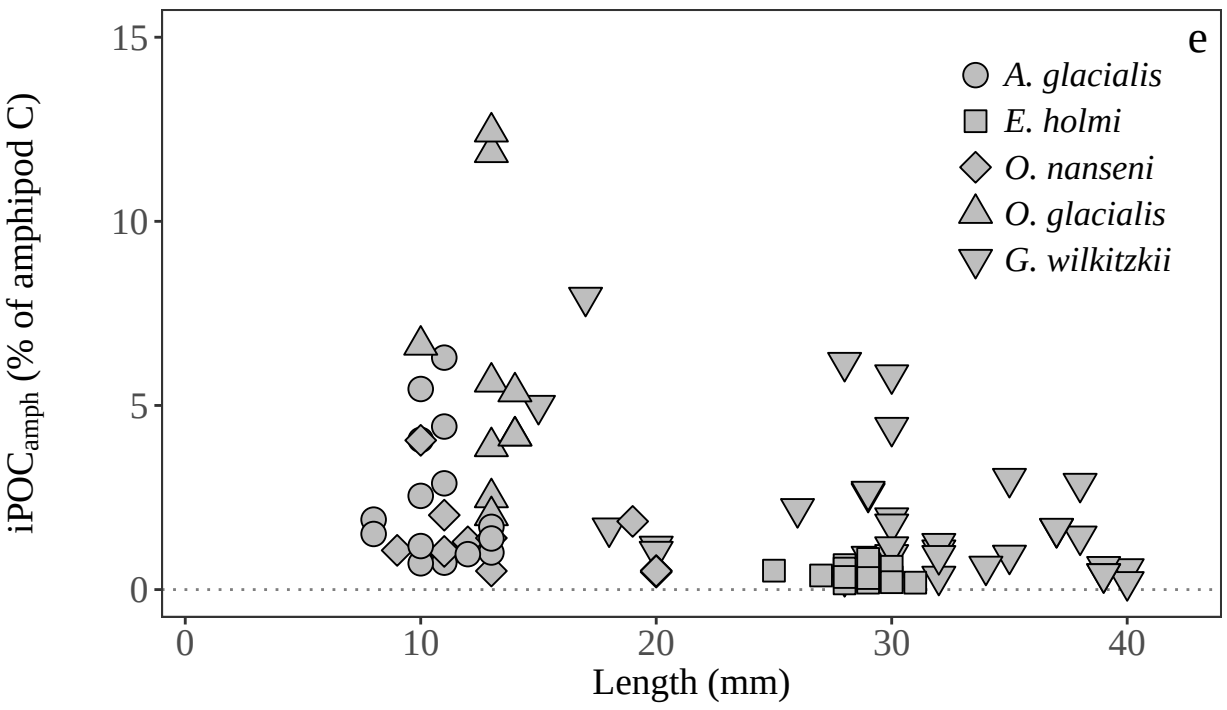

f

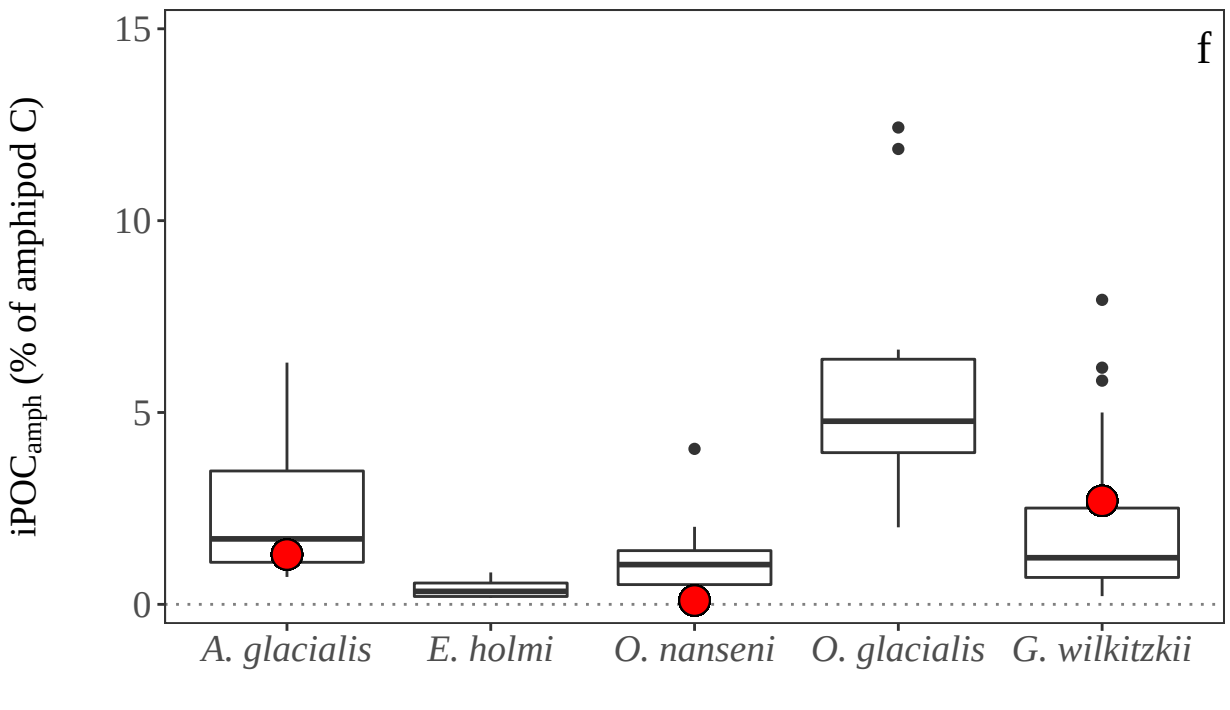

g

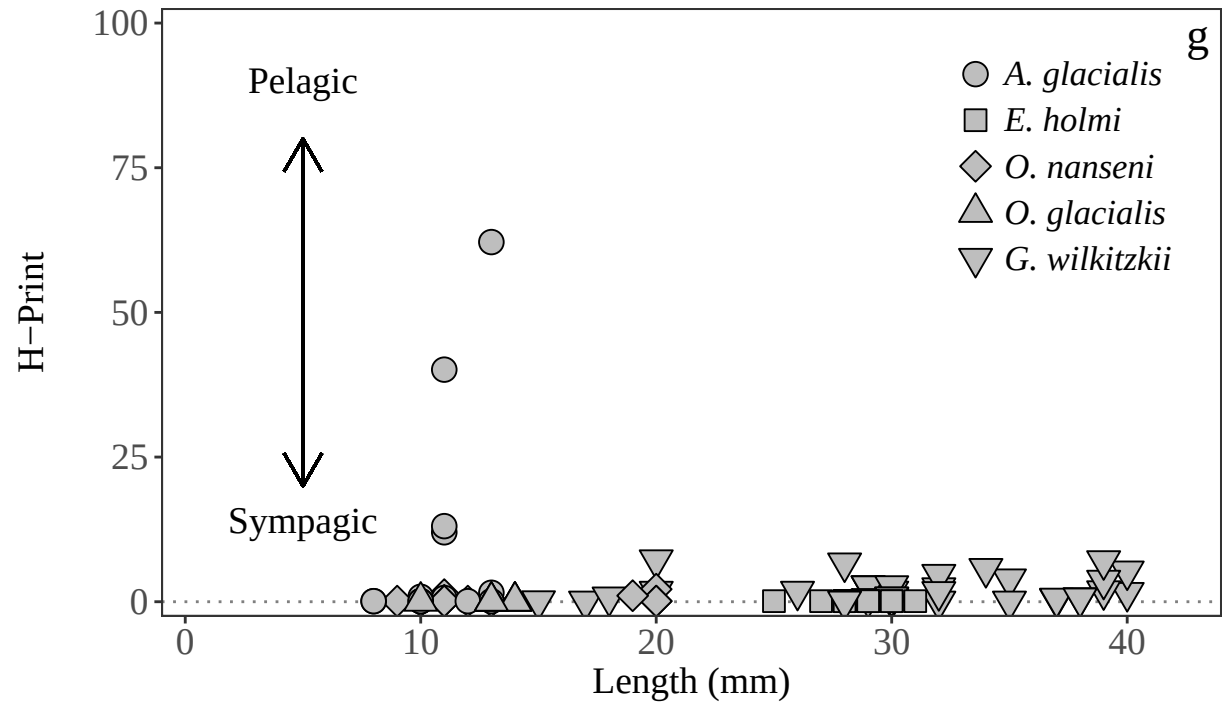

h